Cancer Immunology, Immunotherapy (2021) 70:1015–1029
https://doi.org/10.1007/s00262-020-02741-2

ORIGINAL ARTICLE

OSCC cell-secreted exosomal *CMTM6* induced M2-like macrophages polarization via ERK1/2 signaling pathway

Xin Pang[1] · Sha-sha Wang[1] · Mei Zhang[1] · Jian Jiang[2] · Hua-yang Fan[1] · Jia-shun Wu[1] · Hao-fan Wang[1] · Xin-hua Liang[1] · Ya-ling Tang[1]

Received: 24 April 2020 / Accepted: 12 October 2020 / Published online: 26 October 2020

Abstract

Background *CKLF-like MARVEL transmembrane domain-containing 6* (*CMTM6*) is a critical regulator of tumor immunology among various cancers. However, the role and underlying molecular mechanism of *CMTM6* in oral squamous cell carcinoma (OSCC) progression remains unclear.

Methods The expression of *CMTM6*, *PD-L1* and *CD163* in OSCC tissues were detected by immunohistochemistry on tissue microarray. The effect of *CMTM6* knockdown on OSCC cells and macrophage polarization were analyzed by CCK-8 assay, apoptotic assay, would-healing assay, transwell assay and qPCR. OSCC cell derived exosomes were obtained by ultracentrifugation and the mechanistic studies were conducted by qPCR and Western Blot. 4-Nitroquinoline N-oxide (4NQO) induced OSCC mice were used for verifying the effect of *CMTM6* downregulation on M2 macrophage infiltration and tumor growth.

Results In OSCC samples, higher *CMTM6* expression has been obviously associated with higher pathological stage of OSCC patients, *CD163* + macrophages infiltration and *PD-L1* expression. *CMTM6* knockdown of OSCC cells inhibited proliferative, migrative and invasive abilities of OSCC cells, as well as inhibited M2 macrophage polarization in vitro with downregulating *PD-L1* expression. Importantly, exosomes from OSCC cells shuttled *CMTM6* to macrophages and promoted M2-like macrophage polarization through activating ERK1/2 signaling. In addition, in 4NQO-induced OSCC mice, *CMTM6* level was positively associated with *CD163*, *CD206* and *PD-L1* as well as M2-like macrophage infiltration.

Conclusion OSCC cell-secreted exosomal *CMTM6* induces M2-like macrophages polarization to promote malignant progression via ERK1/2 signaling pathway, revealing a novel crosstalk between cancer cells and immune cells in OSCC microenvironment.

Keywords Oral squamous cell carcinoma · *CKLF-like MARVEL transmembrane domain-containing 6* · Macrophage · Exosome · *PD-L1*

Introduction

Oral squamous cell carcinoma (OSCC) is the most common malignancy of oral cancers, and results in more than 145 thousand mortality annually overworld [1]. Traditional treatment options such as surgery, radiotherapy and chemotherapy failed to improve the 5 year survival rate yet, which is about 50% [2, 3]. In the United States, the estimated numbers of new cases and deaths of OSCC have increased in 2019 [4], emphasizing the need to better understand molecular mechanisms underlying the progression of OSCC to identify new therapeutic targets.

CKLF-like MARVEL transmembrane domain-containing 6 (*CMTM6*), a protein at the plasma membrane, recently has been identified to regulate *PD-L1* expression

Xin Pang, Sha-sha Wang and Mei Zhang contributed equally to this work.

✉ Xin-hua Liang
lxh88866@scu.edu.cn

✉ Ya-ling Tang
tangyaling@scu.edu.cn

[1] State Key Laboratory of Oral Diseases and National Clinical Research Center for Oral Diseases and Department of Oral and Maxillofacial Surgery, Hospital of Stomatology, Sichuan University, No.14, Sec. 3, Renminnan Road, Chengdu 610041, West China, China

[2] Department of Head and Neck Surgery, Sichuan Cancer Center, School of Medicine, Sichuan Cancer Hospital and Institute, University of Electronic Science and Technology of China, Chengdu, Sichuan, China

of tumor cells and limit antitumor immunity [5, 6]. And in the cancer genome atlas (TCGA) databases, *CMTM6* is overexpressed in all samples from 30 cancer types, including cervical squamous cell carcinoma, oesophageal cancer, lung squamous cell carcinoma and head and neck squamous cell carcinoma (HNSCC) [6]. Recent evidence shows that *CMTM6* expression was associated with high malignant gliomas as its expression was positively related to malignant characteristics with frequently genomic aberrations of driver oncogenes in gliomas [7]. And *CMTM6* was also highly expressed in type II and III renal clear cell carcinoma, of which the overall survival was smaller than type I [8]. And polymorphisms of *cmtm6* gene have also observed to in HCC of a southern Chinese population, which may contribute to genetic susceptibility of HCC [9]. However, *CMTM6* was downregulated in hepatocellular carcinoma (HCC) tissues and correlated with metastasis and prognosis of HCC patients [10]. Hence, much is needed to address the molecular mechanisms of *CMTM6* regulating cancer cells, especially OSCC cells.

Macrophages are pivotal drivers of tumor permissive inflammatory microenvironment that contribute to the proliferation and invasion of tumor cells, induce angiogenesis and block anti-tumor immune responses [11]. Tumor-associated macrophages (TAM), which are polarized from M1-like antitumor phenotype to M2-like pro-tumor phenotype, have been demonstrated to increase within many human solid tumors and are related with prognosis [12]. Especially, the infiltration of M2 polarized macrophages has been suggested to be positively correlated with poor prognosis in early-stage OSCC [13, 14]. M2 macrophages produce immunosuppressive cytokines such as *interleukin-10* (*IL-10*) and *arginase-1* (*Arg-1*) to block antitumor immunity, and express a high level of *programmed death ligand 1* (*PD-L1*, also known as *CD274*) in many cancers such as HCC, pancreatic cancer as well as OSCC, thus triggering checkpoint blockade of *T* cells and contributing to immunosuppression towards tumor cells [15–18]. However, the role and significance of *CMTM6* in OSCC contributing to M2-like macrophage polarization remains absent.

Here, we demonstrated that *CMTM6* expression was positively associated with *CD163*$^+$ macrophages infiltration, *PD-L1* expression and tumor stage in OSCC clinical samples and 4NQO-induced oral carcinoma model of mice. And knockdown of *CMTM6* inhibiting proliferation, migration and invasion of OSCC cells was also observed. In addition, a coculture system was established to demonstrate that *CMTM6* increased M2-like macrophage polarization through OSCC-derived exosomes dependent on ERK1/2 signaling in macrophages. Taken together, our results showed that *CMTM6* contributed to OSCC progression, partly by inducing M2 macrophage polarization, which may offer a new insight into OSCC treatment.

Materials and methods

Patients and tissue microarray (TMA)

Paraffin-embedded tumor samples were from patients diagnosed as OSCC from department of oral and maxillofacial surgery, West China Hospital of Stomatology, Sichuan University between 2010 and 2015 and without any preoperative treatments including surgery, radiotherapy or chemotherapy before surgery. Informed consent was obtained from all the patients. 5 normal oral epithelial tissues and 45 OSCC tissues were cored and transferred to the recipient master block.

Animals and ethics statement

All animal experiments were processed as per procedures which approved by the subcommittee on research and animal care (SRAC) of Sichuan University. 6-week-old female wide-type C57BL/6 mice (Dashuo, China) were housed under standard laboratory conditions in state key laboratory of oral diseases, West China Hospital of Stomatology. 4NQO (Sigma, United States) was dissolved to the drinking water at 100 μg/mL for 10 weeks and changed to distilled water for another 10 weeks. Then, the mice were randomly divided into two groups for intratumor injections every 3 days.

Before injection, mice were anesthetized by intraperitoneally injecting a solution with ketamine (80 mg/ml) and xylazine (10 mg/ml). For each local injection, 5 μg *CMTM6* siRNA or negative control siRNA was mixed with 5 μl transfection reagent (Entranster-in vivo, Engreen, China). siRNA target sequence for mouse *CMTM6*: 5′-UGCCUA ACAGAAAGCGUGUTT-3′. After 3 weeks injection, mice were sacrificed by cervical vertebra luxation and the tumor volumes were measured by a caliper. Tumor volume = (length × width^2)/2.

Immunohistochemistry

Immunohistochemistry staining of OSCC tissues was performed as described previously [9]. Briefly, samples were incubated with hydrogen peroxide and serum in turn after dewaxing and dehydration with gradient ethanol. Then, specimens were incubated with anti-*CMTM6* antibody (ZENBIO, China, 1:100), anti-*CD163* antibody (Proteintech, China, 1: 1500) and anti-*PD-L1* (Proteintech, China, 1:300) at 4 °C overnight, washed and then incubated with horseradish peroxidase labeled streptavidin and biotin labeled secondary antibody. All the sections were stained with DAB and were hematoxylin counterstained.

The immunohistochemical result quantification was performed and the subcellular localization (nuclear, cytoplasm,

cell membrane) was identified, respectively. 5 microscopic fields at 400 × magnification per section were observed and the positive cell ratio in tumor cells or stromal cells was estimated. For *CMTM6*, *PD-L1* and *CD163*, the strongly positive expression, moderately positive expression, weakly positive expression and negative expression were categorized into (+++), > 50%; (++), 25–50%; (+), 5–25%; (−), < 5%.

Cell culture and treatment

The human OSCC cell line Cal-27 and SCC25, the human monocytes cell line *THP-1* were from state key laboratory of oral diseases (West China Hospital of Stomatology, Sichuan University). Cal-27 and SCC25 cells were cultured in DMEM medium (HyClone, USA) and F12 medium (HyClone, USA) respectively, and *THP-1* cells were maintained in complete RPMI1640 medium (HyClone, USA). All these cells were cultured with 10% FBS and kept under 5% CO_2 at 37 °C.

Macrophage polarization and coculture

THP-1 cells were seeded at the lower compartment with 100 ng/ml phorbol myristate acetate (PMA). After 48 h, macrophages were washed with PBS in prepare. The Cal-27 or SCC25 cells were seeded into the upper compartment of the Transwell (Millipore, USA) coculture system. Then, the upper and lower compartments were combined with complete RPMI1640 medium with 10% FBS for another 48 h in a humidified chamber. In order to generate well-differentiated M1 macrophages, PMA-differentiated *THP-1* cells were cultured with IFN-γ (20 ng/mL) and LPS (100 ng/mL) for another 48 h. And to obtain well-differentiated M2 macrophages, PMA-differentiated *THP-1* cells were cultured with *IL-4* (20 ng/mL) and *IL-13* (20 ng/mL) for another 48 h.

Cell transfection

The siRNAs sequence 5′-GCUGCAAUUGUGUUUGGAUTT-3′ targeting human *cmtm6* or control siRNA were transiently transfected using Lipofectamine 2000 transfection reagent (GeneCopoeia, US) according to the manufacturer's instructions for siRNA transfection. 24 h later, the transfected cells were collected for further research.

CCK-8 assays

The proliferation of Cal-27 and SCC25 cells was evaluated with CCK-8 assays (Dojindo, China) after transfection. In brief, the plate was washed and added with a 100 μL serum-free medium with 10 μL CCK-8 reagent at 24 h, 48 h and 72 h after transfection, respectively. The absorbance was measured at 450 nm after incubation for 30 min.

Would healing assays

Cal-27 or SCC25 cells were seeded on six-well plates and transfected. Then, a wound across the wall was introduced. After washing with PBS, the plate was incubated with serum-free medium for 24 h. Cell migration was observed and photographed by microscopy.

Apoptosis assays

Cal-27 or SCC25 cells were collected at the time of 24 h and 48 h after transfection. 5 μL Annexin V-FITC (KeyGEN, China) was added to the cell suspension for staining in the dark. After that, 5 μL PI (KeyGEN, China) was applied. Cells were then analyzed by Flow Cytometer.

Invasion assays

Invasion assays were conducted using an 8 μm pore Transwell filter (Corning, US) coated with Matrigel matrix. Cal-27 or SCC25 cells were seeded in the upper chamber with DMEM/F12 serum-free medium. And medium with 20% FBS was added to the lower chamber. After incubation for 48 h, the Transwell filter was washed, fixed with 5% glutaraldehyde and in turn stained with 0.1% crystal violet staining solution.

RNA extraction and reverse transcription-PCR (qPCR) analysis

Total RNA of OSCC cells and *THP-1*-derived macrophages were extracted using total RNA extraction kit (Solarbio, China). Synthesis of cDNA was performed using PrimeScript RT reagent Kit with gDNA Eraser (Takara, Japan) according to manufacturer's instructions. Then, the samples were analyzed in PowerUp SYBR green master mix system (ABI, US). *GADPH* mRNA levels were used to normalize relative mRNA levels. Primer sets used were as follows: *GAPDH* (human), forward 5′-ACAACTTTGGTATCGTGGAAGG-3′, reverse 5′-GCCATCACGCCACAGTTTC-3′; *CMTM6* (human), forward 5′-ATGAAGGCCAGCAGAGACAG-3′, reverse 5′-GTGTACAGCCCCACTACGGA-3′; *CD163* (human), forward 5′-TTTGTCAACTTGAGTCCCTTCAC-3′, reverse 5′-TCCCGCTACACTTGTTTTCAC-3′; *CD86* (human), forward 5′-TGGTGCTGCTCCTCTGAAGATTC-3′, reverse 5′-ATCATTCCTGTGGGCTTTTTGTG-3′; *TNF-α*, forward 5′-GACAAGCCTGTAGCCCATGTTGTA-3′, reverse 5′-CAGCCTTGGCCCTTGAAGA-3′; *IL-12p40*, forward 5′- CGGTCATCTGCCGCAA-3′, reverse 5′-AACCTAACTGCAGGGCACAG-3′;

IL-10, forward 5′- GAGATGCCTTCAGCAGAGTGAAGA -3′, reverse 5′-AGGCTTGGCAACCCAGGTAAC-3′; *Arg-1*, forward 5′- TGGACAGACTAGGAATTGGCA-3′, reverse 5′-CCAGTCCGTCAACATCAAAACT-3′; *SOCS3*, forward 5′- GCTCCAAAAGCGAGTACCAGC-3′, reverse 5′-AGT AGAATCCGCTCTCCTGCAG-3′; *STAT3*, forward 5′-ATC ACGCCTTCTACAGACTGC-3′, reverse 5′-CATCCTGGA GATTCTCTACCACT-3′; *ERK1*, forward 5′- CTACACGCA GTTGCAGTACAT-3′, reverse 5′- CAGCAGGATCTGGAT CTCCC-3′; *ERK2*, forward 5′- TACACCAACCTCTCGTAC ATCG-3′, reverse 5′- CATGTCTGAAGCGCAGTAAGATT-3′; *MIF*, forward 5′- AGCAGCTGGCGCAGGCCAC-3′, reverse 5′- CTCGCTGGAGCCGCCGAAGG-3′; *GADPH* (mouse), forward 5′-GATCCGGGTCCTCAGAGGTTT-3′, reverse 5′-ATCAGGTGGTAGCATAGGCTT-3′; *CMTM6* (mouse), forward 5′-GTGAGCTGTAGCGCCTTTCTC-3′, reverse 5′-TCCGATGACTTGACTTTTCCAG-3′; *CD206* (mouse), forward 5′-CTCTGTTCAGCTATTGGACGC-3′, reverse 5′-CGGAATTTCTGGGATTCAGCTTC-3′; *CD86* (mouse), forward 5′-TCAATGGGACTGCATATCTGCC-3′, reverse 5′-GCCAAAATACTACCAGCTCACT-3′.

Western blotting

Cell or exosomes were lysed with RIPA buffer (Pierce, US) and then centrifuged at 14,000 g for 15 min at 4 °C to collect the supernatants. After mixed with SDS sample buffer, the proteins were heated to 99 °C for 10 min, separated on 10% SDS–polyacrylamide gels, transferred to PVDF membranes, and probed with antibodies against *PD-L1* (1:3000; proteintech, China), p-ERK1/2 (1:1000, Cell Signaling, US), calnexin (1:1000; Affinity, China), *CD63* (1:1000; Affinity, China) and α-tublin (1:2000, Proteintech, China) at 4 °C overnight and blots were visualized using gel imaging systems (Bio-Rad).

Exosome isolation

Cal-27 cells were cultured in DMEM medium with 10% exosome-free FBS. The conditioned medium was collected after 48 h. Then, the exosomes in conditioned medium were isolated by ultracentrifugation. In brief, 40 mL conditioned medium was centrifuged at 300 g for 10 min, 2000 g for 10 min, 10,000 g for 30 min, 100,000 g for 70 min and 100,000 g for another 30 min successively to pellet the exosomes. The final pellet was resuspended in PBS and frozen at − 80 °C.

Exosome uptake

Purified exosomes from supernatant of Cal-27 cells were re-suspended in PBS and labeled by a PKH26 fluorescent kit (Sigma, USA). Briefly, 4 µl PKH26 dye was added to 25 µg exosomes followed by 0.5 ml diluent C and incubated for 5 min at room temperature. They were then mixed with an equal volume of 0.5% BSA. Exosomes labeled with PKH26 were re-isolated as stated above. Finally, the labeled exosomes were incubated with PMA-differentiated *THP-1* cells at 37 °C for 12 h and the fluorescence uptake was observed by the inverted fluorescence microscope. Cal-27 cells incubated with non-labeled exosomes (PBS was added to 25 µg exosomes instead of PKH26) and Cal-27 cells with only PKH26 (PKH26 was added to PBS instead of exosomes and was re-isolated as stated) were used as controls.

Statistical analyses

All experiments were repeated three times independently. Data were analyzed with SPSS 13.0. Statistical significance was designated as $p < 0.05$.

Results

CMTM6 expression is positively associated with CD163 + macrophages infiltration and clinical characteristics in OSCC patients

A tissue microarray containing 5 normal oral mucosa and 45 OSCC tissues was used for *CMTM6*, *CD163* and *PD-L1* immunochemistry staining. Clinic characteristics of 45 OSCC patients were shown in Table 1. The data showed that *CMTM6* were positively stained in plasma membrane or cytoplasm of tumor cells, and was markedly overexpressed in 91.1% cases of OSCC (41/45), compared with 20% (1/5) cases of normal oral mucosa (Fig. 1a). And the strongly, moderately and weakly positive rate was 33.3% (15/45), 44.4% (20/45) and 13.3% (6/45), respectively (Table. 1

Table 1 The expression of *CMTM6* in normal oral mucosa and OSCC

	Cases	Normal ($n=5$)	OSCC ($n=45$)	p value
CMTM6	−	4	4	0.001
	+	1	6	
	++	0	20	
	+++	0	15	

(−), < 5% negative expression; (+), 5–25% weakly positive expression; (++), 25–50% moderately positive expression; (+++), > 50% strongly positive expression

*$p < 0.05$ was regarded as statistically significant in rank sum test

and Fig. 1b). And the expression of *CMTM6* was positively related to *T* stage, pathological grade and lymph node metastasis of OSCC patients ($p<0.05$), but not to the age or gender of patients ($p>0.05$) (Table 2).

Next, the relationship between *CMTM6* with *CD163* + macrophages infiltration and *PD-L1* expression was evaluated. *CD163* + macrophages were heterogeneously located at the tumor stroma, with partial expression at the epithelium. Higher *CD163* + macrophages distribution was significantly detected in *CMTM6* positive OSCC compared to *CMTM6* negative OSCC (Fig. 1c). Furthermore, the intensity of *CD163* + macrophages of *CMTM6*-positive OSCC was also stronger in *CMTM6*-positive OSCC compared to *CMTM6*-negative OSCC (moderate to dense, 84.85% vs. 27.27%) (Fig. 1d). Spearman correlation coefficient test suggested that the intratumoral *CD163* + macrophages density was closely related to *CMTM6* expression ($r=0.595$, $p<0.001$) (Fig. 1c). And the positive expression of *PD-L1* was in the cytoplasm of tumor cells, and was associated with *CMTM6* expression ($r=0.288$, $p<0.05$) (Fig. 1c and 1d). The data were in accordance with the results in tumor immune estimation resource (TIMER) databases that the infiltration of macrophages as well as the expression of *CD163* and *PD-L1* were positively associated with *CMTM6* expression in HNSCC cases through RNA-seq (Fig. 1e). Together, these data implicated that *CMTM6* overexpression indicated poor clinicopathological characteristics, and was positively related to *CD163* + macrophage infiltration and *PD-L1* expression.

CMTM6 knockdown in OSCC cells mitigates OSCC cancer progress with *PD-L1* downregulation

To investigate the potential function of *CMTM6* in OSCC cells, we established three independent siRNAs to knockdown *CMTM6* in Cal-27 and SCC25 cells and siRNA 3 stably downregulated the mRNA and protein levels of *CMTM6* at 24 h after transfection (Fig. 2a). As shown in Fig. 2b, Cal-27 and SCC25 cells proliferation were decreased after silencing CMTM6. Cellular migration and invasion were inhibited in both Cal-27 and SCC25 cells after transfection with si-*CMTM6* (Fig. 2d, e). However, the apoptosis of Cal-27 and SCC25 cells was not affected by transfection of si-*CMTM6* (Fig. 2c). Moreover, *CMTM6* knockdown dramatically reduced the protein level of *PD-L1* in OSCC cells (Fig. 2a). Thus, these indicated that *CMTM6* knockdown could dramatically inhibit the proliferation, migration and invasion of OSCC cells to mitigate OSCC progression with downregulating PD-L1 expression.

CMTM6 in OSCC cells contributes to M2-like macrophage polarization

After obtaining the effect of *CMTM6* on promoting OSCC malignancy, we then analyzed whether it could promote the M2-polarized macrophages, which played an important role in immunity microenvironment facilitating OSCC progression [13]. PMA-differentiated human *THP-1* monocytes (M0 macrophages) were cocultured with OSCC cells using a Transwell system (Fig. 3a), and the expression of M1 and M2 macrophage markers were examined by qPCR. The expression of *CD163* was lower in M0 macrophages with si-*CMTM6* OSCC cells than that with si-NC OSCC cells (Fig. 3b); meanwhile the M1 markers such as *CD80* and *CD86* were increased (Fig. 3c). The mRNA levels of *tumor necrosis factor α (TNF-α)* and *IL-12p40* (M1 cytokines) were markedly upregulated in M0 macrophages in responses to coculture with *CMTM6*-silencing OSCC cells in a variable extent (Fig. 3c). While *CD163* + macrophages were decreased in M0 with si-*CMTM6* Cal-27 cells compared to that with si-NC Cal-27 cells as shown in Fig. 3d (Fig. 3d). And M2 representative gene *IL-10* and *Arg-1* were lower in macrophages induced by si-*CMTM6* OSCC cells than that induced by si-NC OSCC cells (Fig. 3b). Together, these findings indicated that *CMTM6* may be an inducer of M2-like macrophages polarization in OSCC microenvironment.

OSCC cells shuttle *CMTM6* to macrophages through exosomes

We next explored the molecular mechanisms that OSCC cells employed to modulate macrophages polarization. Considering the indirect coculture system conducted, the direct cell-to-cell contacts dependent on cytoskeletal remodeling is excluded. Then, we investigated whether OSCC cells could regulate macrophages polarization through exosomes, which is a crucial mediator in intercellular communication [19]. The exosomes from OSCC cell culture supernatants were extracted through ultracentrifugation (Fig. 4a). Subsequently, we detected the expression of exosome marker *CD63*, *CD9* and *CD81*, as well as endoplasmic reticulum protein calnexin by Western blot (Fig. 4b). *CD63*, *CD9* and *CD81* were positively expressed in exosomes, while calnexin was confirmed absent. Additional, Cal-27 cell lysates were positive for calnexin, suggesting that the exosomes from Cal-27 cells were purified without endoplasmic reticulum vesicles. Thus, we concluded the vesicles we extracted from Cal-27 cell supernatant were purified exosomes.

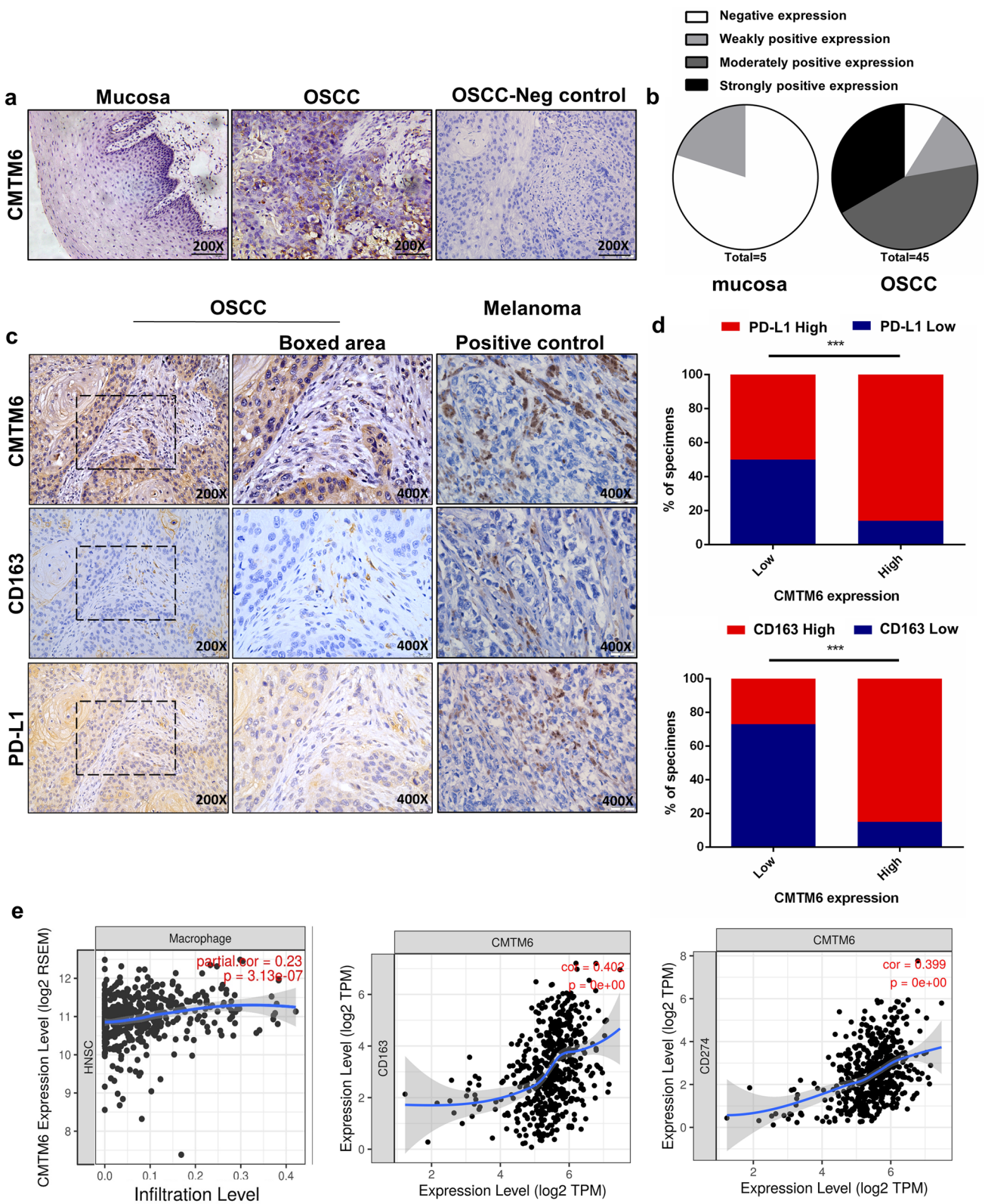
a
Mucosa
OSCC
OSCC-Neg control
CMTM6
200X
b
Negative expression
Weakly positive expression
Moderately positive expression
Strongly positive expression
Total=5
Total=45
mucosa
OSCC
c
OSCC
Melanoma
Boxed area
Positive control
CMTM6
CD163
PD-L1
200X
400X
d
PD-L1 High
PD-L1 Low
***
% of specimens
Low
High
CMTM6 expression
CD163 High
CD163 Low
e
Macrophage
partial.cor = 0.23
p = 3.13e-07
CMTM6 Expression Level (log2 RSEM)
HNSC
Infiltration Level
CMTM6
cor = 0.402
p = 0e+00
Expression Level (log2 TPM)
CD163
cor = 0.399
CD274

◂**Fig. 1** Representative immunohistochemical images of oral mucosa and OSCC sections. **a** Representative images of *CMTM6* immunohistochemical expression and negative control (PBS was added instead of primary antibodies in OSCC tissue microarrays (scale bar: 100 μm). **b** Histoscores for *CMTM6* expression in oral mucosa and OSCC sections. **c** Representative images of OSCC tissues stained for *CMTM6*, *PD-L1* and *CD163* (scale bar: 100um and boxed area scale bar: 50 um) and melanoma tissues stained for *CMTM6*, *PD-L1* and *CD163* for positive control (scale bar: 50 um). **d** Percentage of specimens showing low or high *CMTM6* expression in relation to the expression levels of *PD-L1* and *CD163*. The Chi square test was used to analyze statistical significance. **e** Analyzes of Tumor IMmune Estimation Resource (TIMER) databases showed the association between CMTM6 expression with macrophages infiltration and *CD163*, *PD-L1* expression based on RNA-seq in head and neck squamous cell carcinoma (HNSCC). $*p<0.05$, $**p<0.01$, $***p<0.001$

Then, we explored the possibility that *CMTM6* could be shuttled to macrophages via OSCC cell secreted exosomes. The absorption of OSCC cell-secreted exosomes by macrophages was demonstrated by fluorescence microscopy. We labeled the exosomes with PKH26 and incubated them with M0 for 12 h. Figure 4d shows that the fluorescence signals of PKH26 were dispersed in the cytoplasm of macrophages, demonstrating the OSCC cell-derived exosomes could be efficiently internalization and diffusion in macrophages. Importantly, using Western blot, we found that *CMTM6* was contained in exosomes derived from OSCC cells and could be detected in M0 cells after incubating with OSCC-exosomes (Fig. 4b, c). These results implied *CMTM6* could be shuttled to macrophages through OSCC cells-derived exosomes.

CMTM6 in OSCC cells modulates M2-like macrophage polarization through activating ERK1/2 signaling

ERK1/2 signaling has been known to be related with the polarization of macrophages [20]. Therefore, we asked whether ERK1/2 signaling is involved in the regulation of macrophages by *CMTM6* in OSCC cells. Intriguingly, M0 cocultured with si-*CMTM6* Cal-27 resulted in downregulation of both total and phosphorylated ERK1/2 (Fig. 5b). But the mRNA levels of *SOCS3* (inhibitor of STAT3 signaling), *p38* and macrophage migration inhibitory factor (MIF) were not affected (Fig. 5a). Besides, pre-treatment of OSCC cell with GW4869 (the inhibitor of exosomes) could reduce M2-like macrophages (Fig. 5c). To investigate whether ERK1/2 signaling resulted in M2 polarization, Honokiol, an ERK1/2 activator, was applied to M0 with si-*CMTM6* OSCC cells coculture. As seen in Fig. 5d, M1-like macrophage polarization was largely blocked by honokiol as assessed by the mRNA levels of M1 representative genes *TNF-α* and *IL-12p40*, and the mRNA levels of M2 representative genes *IL-10* and *Arg-1* were increased. Taken together, the results showed that exosomal *CMTM6* of OSCC cells promotes M2 polarization through activating ERK1/2 signaling in macrophage.

CMTM6 silencing inhibits tumor growth and decreases TAM infiltration in 4NQO-treated mice

To confirm the in vitro findings shown above, a 4NQO-induced oral carcinoma model was performed as described previously [21]. si-*CMTM6* or si-NC was mixed with in vivo transfection reagent, and locally injected into the tumor mass every 5 days for 3 weeks. We observed that the tumor volume at the time of sacrifice injected with si-*CMTM6* was markedly less than si-NC ($p=0.0097$, Fig. 6a). In si-*CMTM6* injection group, the average tumor lesion volume was (1.39 ± 0.48) mm^3 and the average lesion number was 2.4 ± 0.4, while the average tumor lesion volume was (8.09 ± 2.31) mm^3 and average lesion number was 4.2 ± 0.4 in si-NC injection group (Fig. 6a). As expected, a lower mRNA levels of *Cmtm6* was found in tumor tissue of si-*CMTM6* injection group compared to control (Fig. 6d). Next, we investigated whether reduced *CMTM6* expression was associated with impaired M2-like macrophage and *PD-L1* expression. Immunohistochemistry analysis showed that tumor samples of si-*CMTM6* injection group exhibited less *CD163* + cells than those in control tumor counterparts, reflecting a smaller number of M2-like macrophages in tumor microenvironment (Fig. 6b, c). And the mRNA levels of M2 macrophage markers *CD163*, *CD206* and *PD-L1* was lower in the tumor samples of si-*CMTM6* injection mice (Fig. 6d). The results also showed that knockdown of *CMTM6* significantly decreased *PD*-L1 expression in 4NQO-treated mice. Therefore, these indicated that disruption of *CMTM6* could block M2-like macrophages in OSCC microenvironment.

Discussion

It is now becoming clear that exosomes travel between cell populations and modify phenotypes of recipient cells in tumor microenvironment. Here, we found that the vesicles we extracted from OSCC cell supernatant were purified exosomes and *CMTM6* could be shuttled to macrophages through OSCC cells-derived exosomes. OSCC-exosomal *CMTM6* facilitated M2 macrophage polarization by activating ERK1/2 signaling. And

Table 2 Clinicopathological features of OSCC patients and their relationship with *CMTM6* expression ($n=45$)

Characteristics	Cases	*CMTM6*		*p* value
		Higher (≥50%)	Lower (<50%)	
Age (years)				
<60	23	18	5	0.780
≥60	22	17	5	
Gender				
Female	16	14	2	0.244
Male	29	21	8	
Tumor size				
T1–T2	16	9	7	0.027*
T3–T4	29	26	3	
Differentiation				
Well or moderate	20	12	8	0.027*
Poor	25	23	2	
Clinical stage				
I–II	13	7	6	0.033*
III–IV	32	28	4	
Nodal metastasis				
Yes	19	18	1	0.048*
No	26	17	9	

*$p<0.05$ was regarded as statistically significant in Chi-square test

CMTM6 promoted migratory and invasive capabilities through enhancing *PD-L1* expression. *CMTM6* was overexpressed in OSCC tissues and was positively related to *CD163* + macrophage infiltration, *PD-L1* expression, as well as clinical pathology. As far as we know, this is the first study to report the roles of *CMTM6* in the crosstalk between cancer cells and immune cells in OSCC microenvironment, which may provide novels insights into tumor treatment on targeting *CMTM6*.

First, we evaluated *CMTM6* expression in OSCC TMA, and found that *CMTM6* was overexpressed in OSCC cells and was positively associated with more advanced stage of OSCC patients. In line with our results, evidences have suggested that *CMTM6* was increased in gliomas and renal clear cell carcinoma [7, 8]. And the highly expression of *CMTM6* has been verified to be associated with high WHO Grade, the IDH wildtype status, as well as predicts poor prognosis in gliomas [7]. Hence, we speculated that *CMTM6* could interact with OSCC cells and facilitate the malignant progression of OSCC. Then, the effect of *CMTM6* on OSCC cells has also been explored. Our results revealed that *CMTM6* depletion resulted in decreased proliferation, migration and invasion of OSCC cells, while the apoptosis of OSCC cells was not affected. In accordance with this, we found that inhibition of *CMTM6* suppressed tumor growth in vivo. And, *CMTM6* interference resulted in impaired *PD-L1* expression of OSCC cancers, which is consistent with Mezzadra et al., who indicated that *CMTM6* silencing significantly impaired *PD-L1* protein expression. These suggested that *CMTM6* could promote OSCC progression through increasing the proliferation, migration and invasion of OSCC cells, with promoting *PD-L1* expression.

It is well known that macrophages are characterized by their plasticity and can mutually transform in response to stimulus in tumor microenvironment. M1 macrophages are generally considered to exert anti-tumor effects in cancers, while M2 macrophages, which are in the majority of TAM, have an opposite function to block antitumor immunity [22]. In gastric and breast cancers, tumor recruiting M2 macrophages was suggested to contribute to tumor progression and metastasis [23, 24]. Here, we demonstrated that $CD163^{+}$ macrophages were highly infiltrated in *CMTM6* overexpressed OSCC samples. Furthermore, *CMTM6* could induced M0–M2-like macrophages dependently on ERK1/2 signaling when cocultured with OSCC cells. In support of these results, inhibition of *CMTM6* resulted in less M2 infiltration in the tumor microenvironment of 4-NQO-induced OSCC tumorigenesis mice. Researches also demonstrated a profound effect of cancer cells on macrophages to effectively evade immune surveillance. For example, Weng et al. showed that oncogene Multiple Copies in *T* cell Malignancy 1 (MCT-1) expression in tumor cells drove M2 macrophage polarization in triple-negative breast cancer [25]. Mu et al. also indicated tumor derived lactate was a pivotal metabolite that promoted M2-like polarization and breast cancer progression [20]. Similarly, pancreatic cancer cells could also potently induce M2 phenotype of RAW264.7 macrophages [26]. Together with our results, we showed that OSCC cells could induce M2-like phenotype through *CMTM6* expression.

Fig. 2 *CMTM6* knockdown inhibited proliferation, migration and invasion of OSCC cells. **a** qPCR and Western blot showing *CMTM6* knockout in Cal-27 cells and *PD-L1* expression in *CMTM6* knockout Cal-27 cells. **b** Cell proliferation of OSCC cells transfected with *CMTM6* siRNA and control siRNA quantified by CCK8 assays. **c** Cell apoptosis of OSCC cells transfected with *CMTM6* siRNA and control siRNA quantified by flow cytometry. **d** Cell migration of OSCC cells transfected with *CMTM6* siRNA and control siRNA quantified by Wound healing assays (scale bar: 200 um). **e** Cell invasion of OSCC cells transfected with *CMTM6* siRNA and control siRNA quantified by Transwell assays (scale bar: 200um). *$p<0.05$, **$p<0.01$, ***$p<0.001$

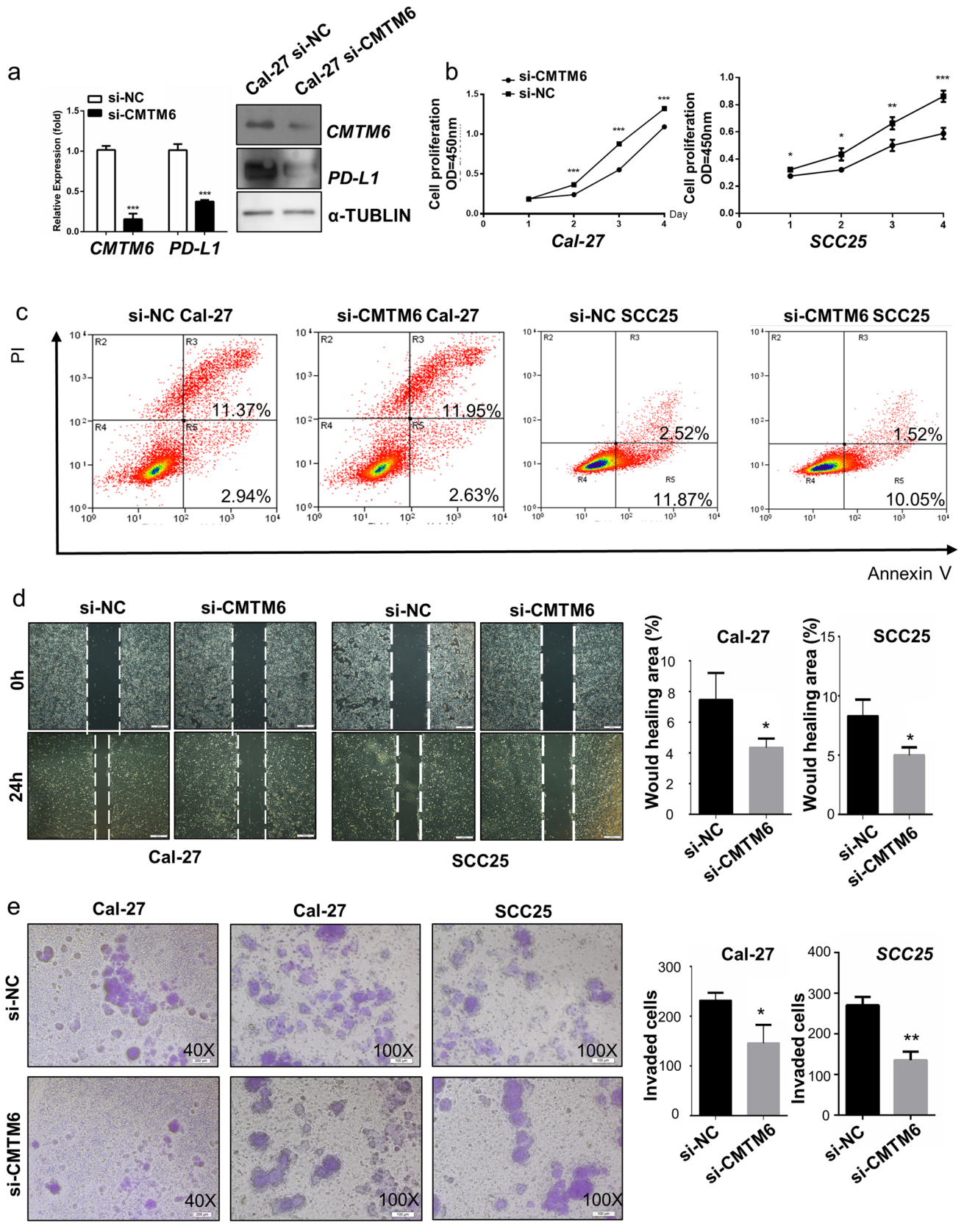
a
si-NC
si-CMTM6
Relative Expression (fold)
CMTM6
PD-L1
Cal-27 si-NC
Cal-27 si-CMTM6
CMTM6
PD-L1
α-TUBLIN
b
si-CMTM6
si-NC
Cell proliferation OD=450nm
Day
Cal-27
SCC25
c
si-NC Cal-27
si-CMTM6 Cal-27
si-NC SCC25
si-CMTM6 SCC25
PI
Annexin V
11.37%
2.94%
11.95%
2.63%
2.52%
11.87%
1.52%
10.05%
d
si-NC
si-CMTM6
0h
24h
Cal-27
SCC25
Would healing area (%)
e
Cal-27
SCC25
si-NC
si-CMTM6
40X
100X
Invaded cells

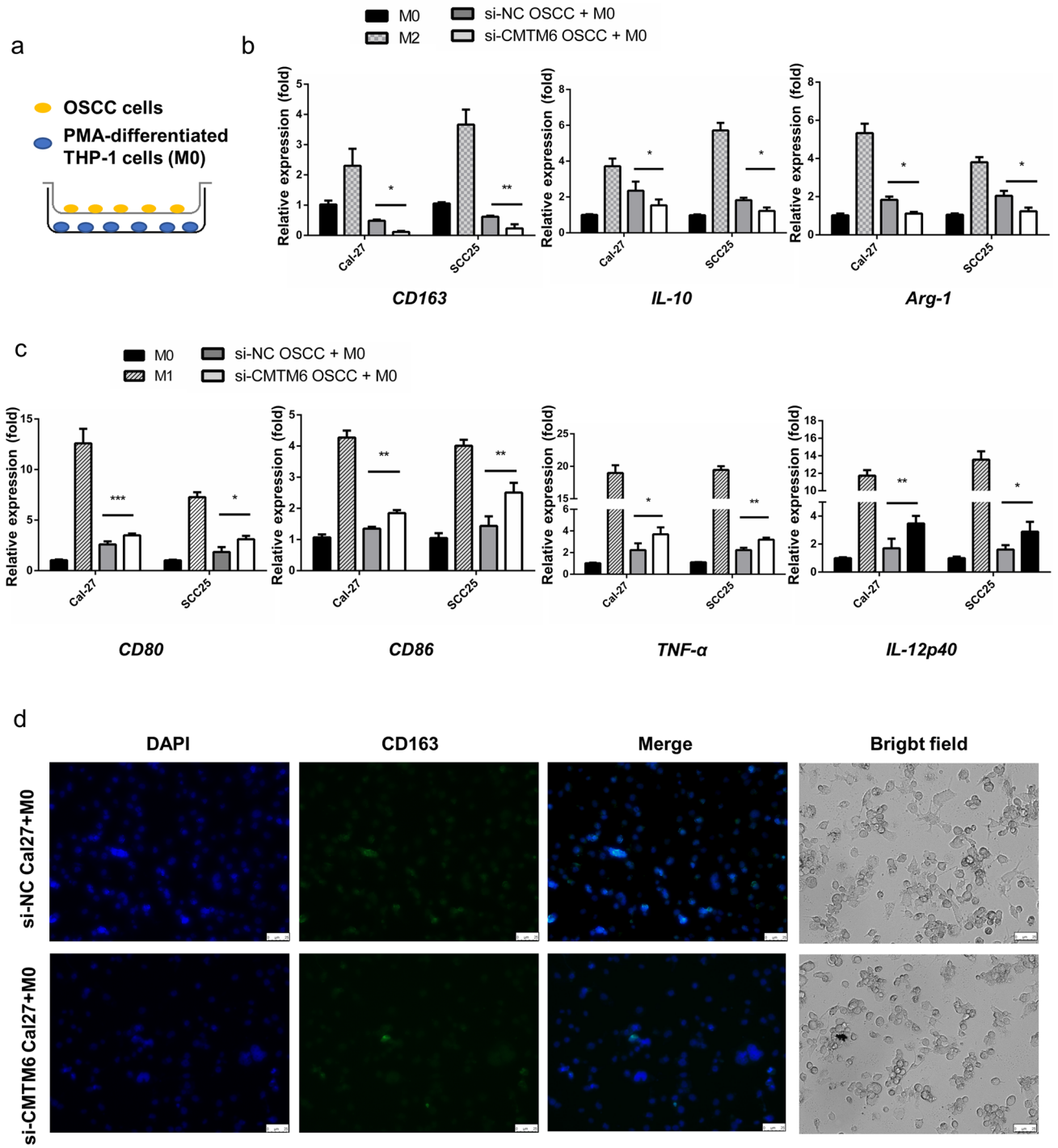

Fig. 3 *CMTM6* inhibition resulted M1-like phenotype polarized in vitro. *THP-1* cells were pre-treated with 100 ng/ml PMA for 48 h before cocultured with Cal-27 cells. **a** A sketch for the Transwell coculture system for PMA-induced THP-1 cells and Cal-27 cells. **b**, **c** qPCR analyses showing mRNA levels of M1 markers (*CD80*, *CD86*, *TNF-α* and *IL-12p40*) and M2 macrophage markers (*CD163*, *IL-10* and *Arg-1*) of M0 cells cocultured with OSCC cells. Results are showed as the relative fold change compared with M0. **d** Immunofluorescent DAPI (blue) and *CD163* (green) staining and the morphology of M0 after coculture (scale bar: 25um). $*p<0.05$, $**p<0.01$, $***p<0.001$

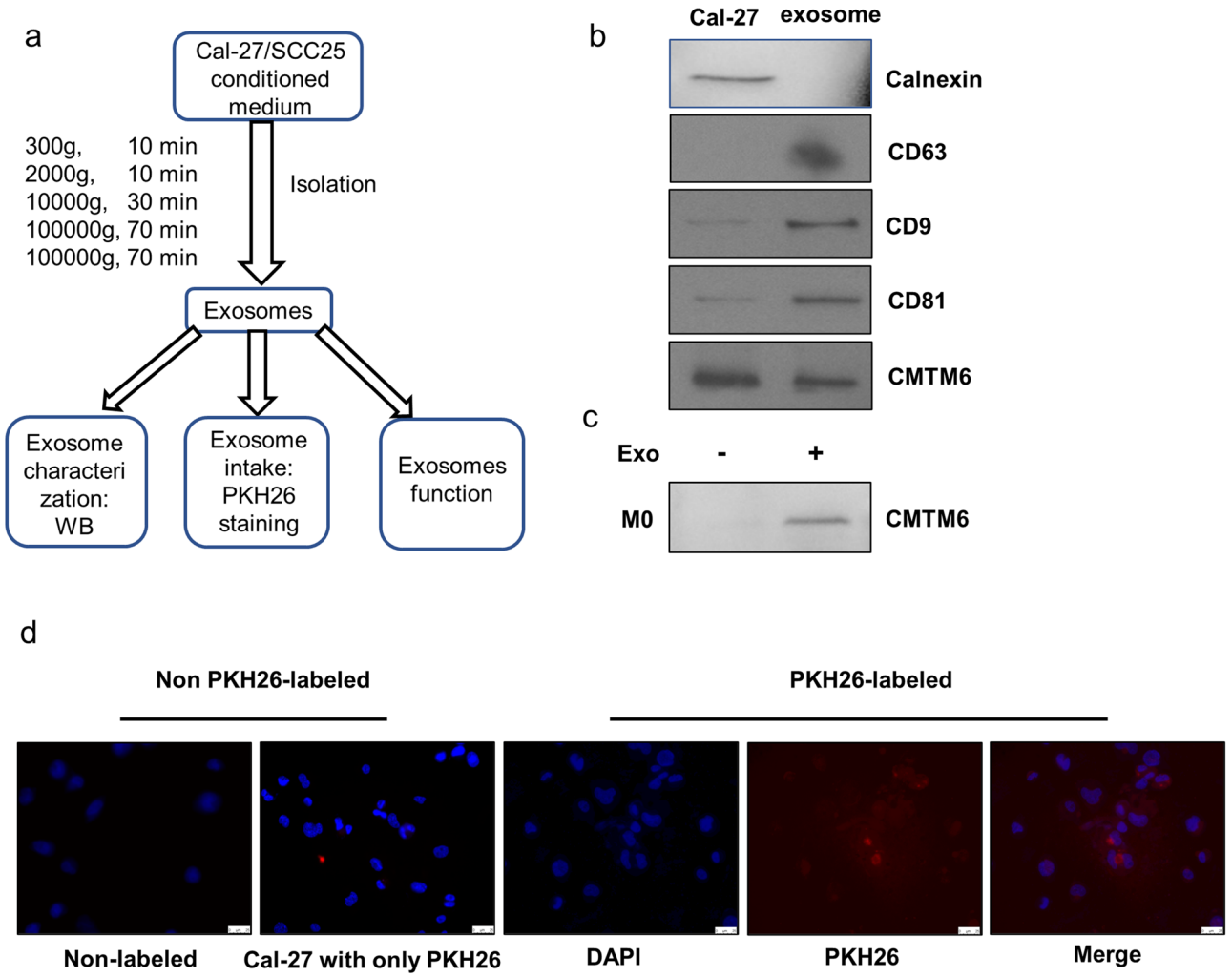

Fig. 4 The isolation and identification of Cal-27 exosomes. **a** A sketch of isolation path and identification of exosomes. **b** Western blot analyzed of exosomes for *CD63*, *CD9* and *CD81* (exosome biomarker), Calnexin (negative marker) and *CMTM6*. **c** Western blot analyzed of M0 cells and exosomes incubated M0 cells for *CMTM6*. **d** Representative fluorescent images for PKH26-labeled exosomes taken by M0 after 12 h incubation. Exosomes were stained red and M0 nuclei were stained blue by DAPI (scale bar: 25um). Cal-27 cells incubated with non-labeled exosomes (PBS was added to 25 μg exosomes instead of PKH26) and Cal-27 cells with only PKH26 (PKH26 was added to PBS and was re-isolated as stated) were used as controls

Exosomes once were thought to remove redundancy from cells. While this has been highlighted recently with increased researches that exosomes were capable to travel between cells and transport signals to recipient cells, thus participating in cancer progression [27]. We found that *CMTM6* could be shuttled by OSCC derived exosomes to M0 and resulted in M2-like polarization in vitro. In accordance with our results, Wang et al. founded that hypoxic exosomal miR-301a-3p from pancreatic cancer cells induced M2 polarization through activating PTEN/PI3Kγ signaling pathway [28]. Similarly, Chen et al. indicated that hypoxia induced high expression of miR-940 in epithelial ovarian cancer (EOC)-derived exosomes to stimulate M2 phenotype polarization, which promoted EOC proliferation and migration [29]. While others suggested that melanoma exosomes did not exclusively polarize macrophages, but induced a mixed M1 and M2 polarization [30]. This indicated *CMTM6* of OSCC cells modulate M2 macrophage polarization through exosomes.

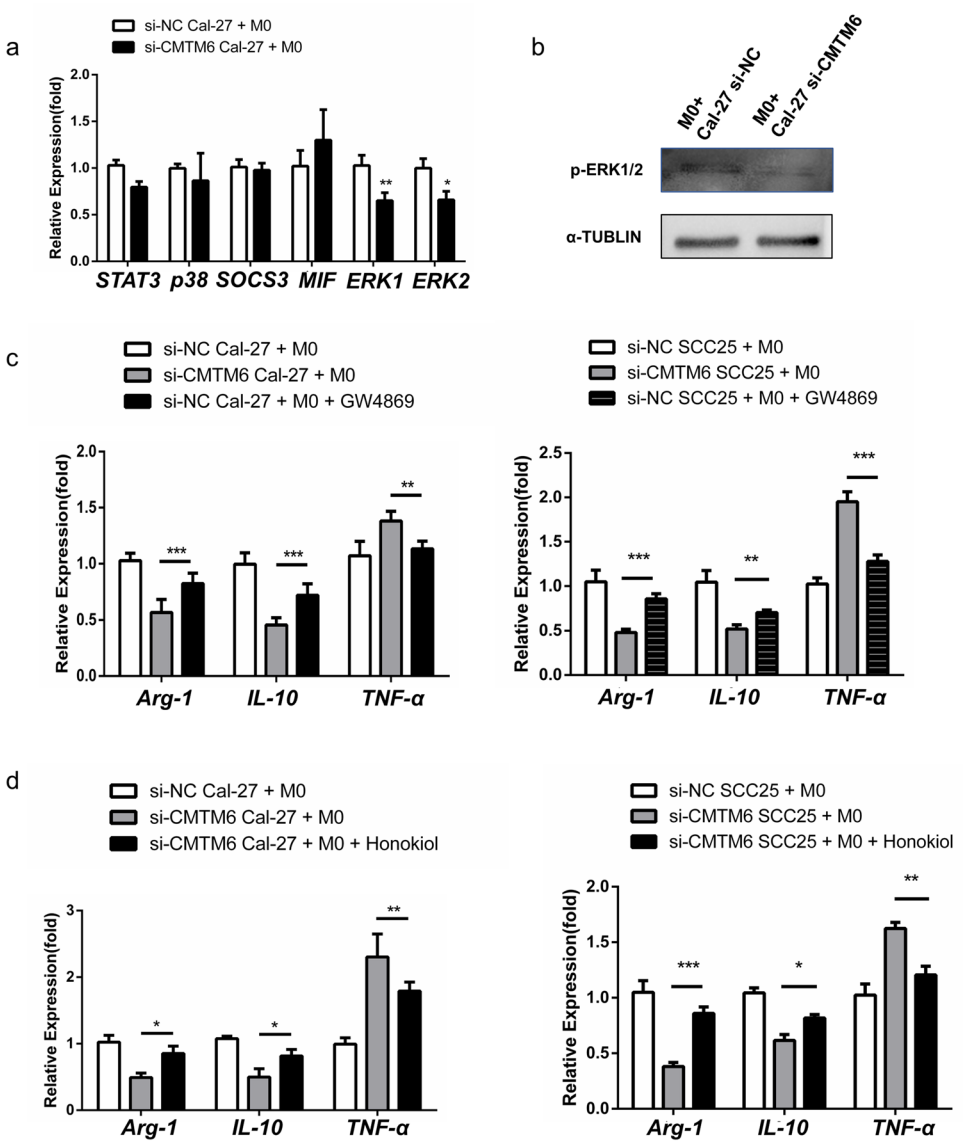

Fig. 5 OSCC exosomes promote M2-like phenotype through activating ERK1/2 signaling. M0 macrophages were cocultured with Cal-27 cells transfected with si-*CMTM6* or control siRNA. **a** The mRNA levels of *STAT3*, *SOCS3*, *MIF*, *p38* and ERK1/2 analyzed by qPCR. **b** The protein levels of p-ERK1/2 analyzed by Western blot. **c** The mRNA levels of M1 markers (*TNF-α* and *IL-12p40*) and M2 markers (*IL-10* and *Arg-1*) after a 48 h coculturing with 10 μM GW4869 pre-treated OSCC cells. **d** The mRNA levels of M1 markers (*TNF-α* and *IL-12p40*) and M2 markers (*IL-10* and *Arg-1*) after a 48-h coculture with or without 5 μM Honokiol

In summary, OSCC cell-secreted exosomal *CMTM6* induced M2-like macrophages polarization via ERK1/2 signaling pathway to contribute to the malignant progression, which involved in mediation of crosstalk between cancer cells and macrophages. Although this signaling pathway concerns complicated immune networks that need to be studied further in detail, targeting *CMTM6* combined with *PD-L1* inhibition or immunotherapy might be a new strategy for OSCC.

Fig. 6 *CMTM6* knockdown blocked OSCC progression and decreased *PD-L1* and *CD163* expression in vivo. **a** Image of tongue tissues (scale bar 1 cm) and the quantitative data of tumor lesion size and lesion number per mouse. **b** Representative HE and immunohistochemical images of tongue tissues, including hyperplasia and carcinoma (scale bar 50 μm). **c** Percentage of specimens showing the expression levels of *PD-L1* and *CD163* in si-NC and si-*CMTM6* group. The Chi-square test was used to analyze statistical significance. **d** The mRNA levels of *CMTM6*, *PD-L1*, *CD86* (M1 marker), *CD163* and *CD206* (M2 marker) in tongue tissues in 4NQO induced oral carcinogenesis mice injected with si-*CMTM6* and control siRNA. **e** Schematic cartoon illustrating that *CMTM6* promoted proliferation, migration and invasion of OSCC cells and induced M2 macrophage polarization through exosomes ▶

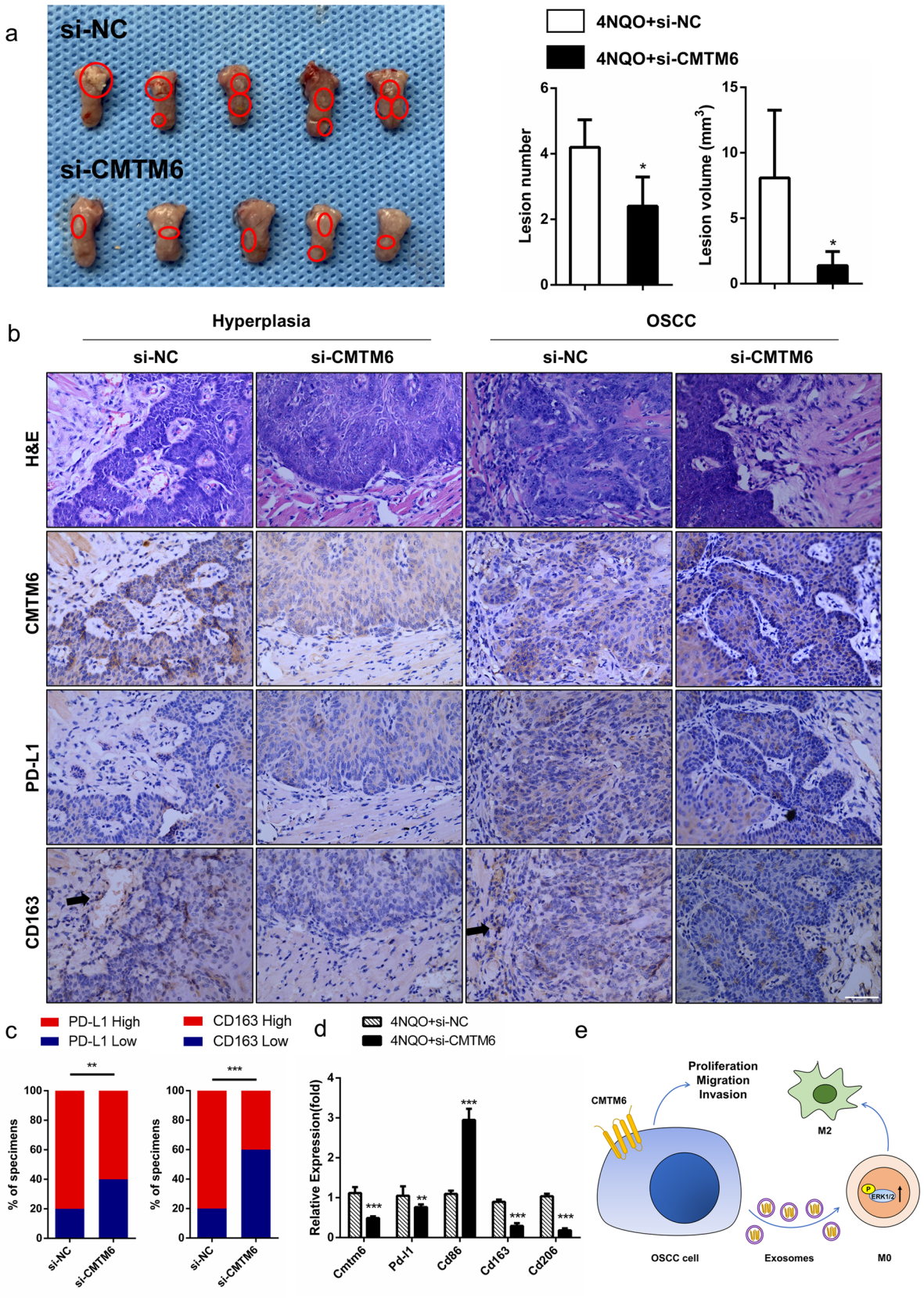
a
si-NC
si-CMTM6
4NQO+si-NC
4NQO+si-CMTM6
Lesion number
Lesion volume (mm3)
b
Hyperplasia
OSCC
si-NC
si-CMTM6
si-NC
si-CMTM6
H&E
CMTM6
PD-L1
CD163
c
PD-L1 High
PD-L1 Low
CD163 High
CD163 Low
% of specimens
si-NC
si-CMTM6
d
4NQO+si-NC
4NQO+si-CMTM6
Relative Expression(fold)
Cmtm6
Pd-l1
Cd86
Cd163
Cd206
e
Proliferation
Migration
Invasion
CMTM6
M2
ERK1/2
OSCC cell
Exosomes
M0

Acknowledgements This work was supported by National Natural Science Foundation of China grants (Nos.8207300, 81672672, 81972542 and 81902779) and National Science Foundation of Sichuan Province (Nos.2020JDRC0018 and 2020YFS0171).

Author contributions Xin Pang, Sha-sha Wang and Mei Zhang performed most of the experiments and wrote the manuscript. Hua-yang Fan and Jia-shun Wu performed the mice materials. Hao-fan Wang analyzed data and assisted in manuscript writing. Xin-hua Liang and Ya-ling Tang conceived the study and performed the final corrections.

Compliance with ethical standards

Conflict of interest The authors declare no conflict of interest.

References

1. Ferlay J, Soerjomataram I, Dikshit R, Eser S, Mathers C, Rebelo M, Parkin DM, Forman D, Bray F (2015) Cancer incidence and mortality worldwide: sources, methods and major patterns in GLOBOCAN 2012. Int J Cancer 136(5):E359-386. https://doi.org/10.1002/ijc.29210
2. Krstevska V (2015) Evolution of treatment and high-risk features in resectable locally advanced Head and Neck squamous cell carcinoma with special reference to extracapsular extension of nodal disease. J BUON 20(4):943–953
3. Pring M, Prime S, Parkinson E, Paterson I (2006) Dysregulated TGF-beta1-induced smad signalling occurs as a result of defects in multiple components of the TGF-beta signalling pathway in human head and neck carcinoma cell lines. Int J Oncol 28(5):1279–1285
4. Siegel RL, Miller KD, Jemal A (2019) Cancer statistics. CA Cancer J Clin 69(1):7–34. https://doi.org/10.3322/caac.21551
5. Burr ML, Sparbier CE, Chan YC, Williamson JC, Woods K, Beavis PA, Lam EYN, Henderson MA, Bell CC, Stolzenburg S, Gilan O, Bloor S, Noori T, Morgens DW, Bassik MC, Neeson PJ, Behren A, Darcy PK, Dawson SJ, Voskoboinik I, Trapani JA, Cebon J, Lehner PJ, Dawson MA (2017) *CMTM6* maintains the expression of *PD-L1* and regulates anti-tumour immunity. Nature 549(7670):101–105. https://doi.org/10.1038/nature23643
6. Mezzadra R, Sun C, Jae LT, Gomez-Eerland R, de Vries E, Wu W, Logtenberg MEW, Slagter M, Rozeman EA, Hofland I, Broeks A, Horlings HM, Wessels LFA, Blank CU, Xiao Y, Heck AJR, Borst J, Brummelkamp TR, Schumacher TNM (2017) Identification of *CMTM6* and *CMTM4* as *PD-L1* protein regulators. Nature 549(7670):106–110. https://doi.org/10.1038/nature23669
7. Guan X, Zhang C, Zhao J, Sun G, Song Q, Jia W (2018) *CMTM6* overexpression is associated with molecular and clinical characteristics of malignancy and predicts poor prognosis in gliomas. EBioMedicine 35:233–243. https://doi.org/10.1016/j.ebiom.2018.08.012
8. Zhao W, Zhao F, Yang K, Lu Y, Zhang Y, Wang W, Xie H, Deng K, Yang C, Rong Z, Hou Y, Li K (2019) An immunophenotyping of renal clear cell carcinoma with characteristics and a potential therapeutic target for patients insensitive to immune checkpoint blockade. J Cell Biochem 120(8):13330–13341. https://doi.org/10.1002/jcb.28607
9. Yafune A, Kawai M, Itahashi M, Kimura M, Nakane F, Mitsumori K, Shibutani M (2013) Global DNA methylation screening of liver in piperonyl butoxide-treated mice in a two-stage hepatocarcinogenesis model. Toxicol Lett 222(3):295–302. https://doi.org/10.1016/j.toxlet.2013.08.006
10. Zhu X, Qi G, Li C, Bei C, Tan C, Zhang Y, Shi W, Zeng W, Kong J, Fu Y, Tan S (2019) Expression and clinical significance of *CMTM6* in hepatocellular carcinoma. DNA Cell Biol 38(2):193–197. https://doi.org/10.1089/dna.2018.4513
11. Singh Y, Pawar VK, Meher JG, Raval K, Kumar A, Shrivastava R, Bhadauria S, Chourasia MK (2017) Targeting tumor associated macrophages (TAMs) via nanocarriers. J Control Release 254:92–106. https://doi.org/10.1016/j.jconrel.2017.03.395
12. Bingle L, Brown NJ, Lewis CE (2002) The role of tumour-associated macrophages in tumour progression: implications for new anticancer therapies. J Pathol 196(3):254–265. https://doi.org/10.1002/path.1027
13. Weber M, Iliopoulos C, Moebius P, Buttner-Herold M, Amann K, Ries J, Preidl R, Neukam FW, Wehrhan F (2016) Prognostic significance of macrophage polarization in early stage oral squamous cell carcinomas. Oral Oncol 52:75–84. https://doi.org/10.1016/j.oraloncology.2015.11.001
14 Biswas SK, Sica A, Lewis CE (2008) Plasticity of macrophage function during tumor progression: regulation by distinct molecular mechanisms. J Immunol 180(4):2011–2017. https://doi.org/10.4049/jimmunol.180.4.2011
15. Kryczek I, Zou L, Rodriguez P, Zhu G, Wei S, Mottram P, Brumlik M, Cheng P, Curiel T, Myers L, Lackner A, Alvarez X, Ochoa A, Chen L, Zou W (2006) B7–H4 expression identifies a novel suppressive macrophage population in human ovarian carcinoma. J Exp Med 203(4):871–881. https://doi.org/10.1084/jem.20050930
16. Winograd R, Byrne KT, Evans RA, Odorizzi PM, Meyer AR, Bajor DL, Clendenin C, Stanger BZ, Furth EE, Wherry EJ, Vonderheide RH (2015) Induction of *T* cell immunity overcomes complete resistance to *PD-1* and *CTLA-4* blockade and improves survival in pancreatic carcinoma. Cancer Immunol Res 3(4):399–411. https://doi.org/10.1158/2326-6066.Cir-14-0215
17. Jiang C, Yuan F, Wang J, Wu L (2017) Oral squamous cell carcinoma suppressed antitumor immunity through induction of *PD-L1* expression on tumor-associated macrophages. Immunobiology 222(4):651–657. https://doi.org/10.1016/j.imbio.2016.12.002
18. Wen ZF, Liu H, Gao R, Zhou M, Ma J, Zhang Y, Zhao J, Chen Y, Zhang T, Huang F, Pan N, Zhang J, Fox BA, Hu HM, Wang LX (2018) Tumor cell-released autophagosomes (TRAPs) promote immunosuppression through induction of M2-like macrophages with increased expression of *PD-L1*. J Immunother Cancer 6(1):151. https://doi.org/10.1186/s40425-018-0452-5
19. Sun LP, Xu K, Cui J, Yuan DY, Zou B, Li J, Liu JL, Li KY, Meng Z, Zhang B (2019) Cancerassociated fibroblastderived exosomal miR3825p promotes the migration and invasion of oral squamous cell carcinoma. Oncol Rep 42(4):1319–1328. https://doi.org/10.3892/or.2019.7255
20. Mu X, Shi W, Xu Y, Xu C, Zhao T, Geng B, Yang J, Pan J, Hu S, Zhang C, Zhang J, Wang C, Shen J, Che Y, Liu Z, Lv Y, Wen H, You Q (2018) Tumor-derived lactate induces M2 macrophage polarization via the activation of the ERK/STAT3 signaling pathway in breast cancer. Cell Cycle 17(4):428–438. https://doi.org/10.1080/15384101.2018.1444305
21. Wu JS, Zheng M, Zhang M, Pang X, Li L, Wang SS, Yang X, Wu JB, Tang YJ, Tang YL, Liang XH (2018) Porphyromonas gingivalis promotes 4-Nitroquinoline-1-Oxide-induced oral carcinogenesis with an alteration of fatty acid metabolism. Frontiers in microbiology 9:2081. https://doi.org/10.3389/fmicb.2018.02081
22. Tong H, Ke JQ, Jiang FZ, Wang XJ, Wang FY, Li YR, Lu W, Wan XP (2016) Tumor-associated macrophage-derived CXCL8 could induce ERalpha suppression via HOXB13 in endometrial cancer. Cancer Lett 376(1):127–136. https://doi.org/10.1016/j.canlet.2016.03.036

23. Yamaguchi T, Fushida S, Yamamoto Y, Tsukada T, Kinoshita J, Oyama K, Miyashita T, Tajima H, Ninomiya I, Munesue S, Harashima A, Harada S, Yamamoto H, Ohta T (2016) Tumor-associated macrophages of the M2 phenotype contribute to progression in gastric cancer with peritoneal dissemination. Gastric Cancer 19(4):1052–1065. https://doi.org/10.1007/s10120-015-0579-8
24. Chen Y, Zhang S, Wang Q, Zhang X (2017) Tumor-recruited M2 macrophages promote gastric and breast cancer metastasis via M2 macrophage-secreted CHI3L1 protein. J Hematol Oncology 10(1):36. https://doi.org/10.1186/s13045-017-0408-0
25. Weng YS, Tseng HY, Chen YA, Shen PC, Al Haq AT, Chen LM, Tung YC, Hsu HL (2019) MCT-1/miR-34a/IL-6/IL-6R signaling axis promotes EMT progression, cancer stemness and M2 macrophage polarization in triple-negative breast cancer. Mol Can 18(1):42. https://doi.org/10.1186/s12943-019-0988-0
26. Khabipov A, Kading A, Liedtke KR, Freund E, Partecke LI, Bekeschus S (2019) RAW 264.7 macrophage polarization by pancreatic cancer cells—a model for studying tumour-promoting macrophages. Anticancer Res 39(6):2871–2882. https://doi.org/10.2187/anticanres.13416
27. Lobb RJ, van Amerongen R, Wiegmans A, Ham S, Larsen JE, Moller A (2017) Exosomes derived from mesenchymal non-small cell lung cancer cells promote chemoresistance. Int J Cancer 141(3):614–620. https://doi.org/10.1002/ijc.30752
28. Wang X, Luo G, Zhang K, Cao J, Huang C, Jiang T, Liu B, Su L, Qiu Z (2018) Hypoxic tumor-derived exosomal miR-301a mediates M2 macrophage polarization via PTEN/PI3Kgamma to promote pancreatic cancer metastasis. Can Res 78(16):4586–4598. https://doi.org/10.1158/0008-5472.Can-17-3841
29. Chen X, Ying X, Wang X, Wu X, Zhu Q, Wang X (2017) Exosomes derived from hypoxic epithelial ovarian cancer deliver microRNA-940 to induce macrophage M2 polarization. Oncol Rep 38(1):522–528. https://doi.org/10.3892/or.2017.5697
30. Bardi GT, Smith MA, Hood JL (2018) Melanoma exosomes promote mixed M1 and M2 macrophage polarization. Cytokine 105:63–72. https://doi.org/10.1016/j.cyto.2018.02.002